Local Order and Chain Dynamics in Molten Polymer Blocks Revealed by Proton Double-Quantum NMR

T. Dollase, R. Graf, A. Heuer, and H. W. Spiess*

Max-Planck-Institut für Polymerforschung, Ackermannweg 10, D-55128 Mainz, Germany

Received August 8, 2000

ABSTRACT: High-resolution proton double-quantum (DQ) magic-angle spinning (MAS) NMR is used as a new technique that is capable of revealing complex motional processes in entangled polymer melts. Theoretical analysis shows the connection of quantities relating anisotropic polymer dynamics to data obtained from our DQ-MAS NMR experiment. With this technique, dynamic chain ordering as well as scaling laws consistent with the reptation model was previously observed for polybutadiene (PB). Here, the influence of rigid confinements represented by immobile moieties attached to one or both chain ends of the PB block on chain dynamics and ordering are investigated. Symmetric poly(styrene-*b*-butadiene) diblock copolymers (PS-*b*-PB) with varying molecular weights are examined as systems with one anchored chain end. As materials with two tethered chain ends PS-*b*-PB-*b*-PS triblock copolymers are studied. In these systems, the effects of rigid confinements on the polymer dynamics in the melt are analyzed. We find that dynamic order parameters are increased by more than a factor of 2 for block copolymers compared to homopolymers. Furthermore, on account of the chemical constraints imposed on the PB block, the lack of the motional regime that involves diffusive reptation motion is experimentally confirmed. Correspondingly, the scaling law pattern differs qualitatively from those observed for PB homopolymers.

1. Introduction

Heterogeneous block copolymers composed of blocks with significantly different glass transitions are interesting thermoplastic elastomers and have been widely studied in academic[1] and industrial research[2] on account of their unique physical and technical properties. For better understanding of these systems, a new comparison of chain dynamics of the molten component of block copolymers with that of the analogous homopolymer melt is particularly informative. Poly(styrene-*b*-butadiene) diblock copolymers (PS-*b*-PB) were chosen for this investigation. 1,4-PB was selected as the mobile phase, since it comprises several interesting features such as a fairly low glass-transition temperature, T_g, which makes it conveniently accessible to experiment. Moreover, if a proper synthetical approach is employed, PB can be prepared nearly as a pure main-chain polymer, avoiding a complex superposition of main-chain and side-group dynamics. PS was chosen as the rigid component in the block copolymers because of its considerably higher T_g, leading to a large temperature range over which the dynamics of the molten PB block can be studied while the PS block remains rigid. Another advantage of using butadiene and styrene as monomers is the fact that well-defined block copolymers with a narrow weight distribution can be prepared via living anionic polymerization. Moreover, from simple ^{1}H NMR measurements, the chain dynamics in PB are known to be anisotropic on intermediate time scales due to restrictions composed by topological constraints (entanglements).[3,4]

Recently, we established a novel technique to study anisotropic chain dynamics of polymers in the melt and in elastomers in a quantitative way.[5,6] Using advanced solid-state nuclear magnetic resonance (NMR) on protons, particularly double-quantum (DQ) magic-angle spinning (MAS) NMR spectroscopy, it became possible to observe main-chain motional processes in PB that could successfully be interpreted in the framework of the reptation model for polymer motion introduced by de Gennes.[7,8] The present investigation extends our preceding work by attaching either one or two rigid blocks to the PB chain ends. This creates structural constraints which strongly affect the translational motion of the PB block. Symmetric poly(styrene-*b*-butadiene), PS-*b*-PB, diblock copolymers of varying molecular weight were chosen as systems with one fixed chain end while PS-*b*-PB-*b*-PS triblock copolymers were selected as systems with two tethered chain ends (Figure 1).

The paper is structured as follows: first the investigated materials will be specified and the experimental NMR technique introduced. Then the formalism that connects NMR results as obtained by our DQ technique with polymer dynamics will be outlined, including a brief review of some fundamental aspects about the reptation model of polymer motion that are needed in our analysis. Finally, our results on local order and main-chain dynamics in PS/PB block copolymers will be discussed and related to the behavior of analoguous PB homopolymer melts and cross-linked styrene-butadiene rubbers (SBR).

2. Experimental Section

2.1. Materials. The PS-*b*-PB diblock copolymers studied were synthesized by living anionic polymerization according to well-established procedures.[9] Use of nonpolar solvent ensured a product distribution of the PB chains of 95% 1,4-butadiene linkage (of which 55% exhibit trans conformation and 45% cis) and 5% 1,2-butadiene linkage, checked by high-resolution ^{1}H and ^{13}C NMR. Because of their enthalpic incompatibility, PS and PB tend to phase separate as predicted by the Flory−Huggins theory.[10,11] Depending on the volume fractions several different morphologies can be formed.[12] For our systems, which are approximately symmetric with respect to molar volume, the existence of lamellae was confirmed by small-angle X-ray scattering (SAXS) and transmission-electron microscopy (TEM). Respective lamellar spacings, L_{exp}, obtained from SAXS along with block lengths, M_n, and glass-

* To whom correspondence should be addressed.

10.1021/ma0013915 CCC: $20.00
Published on Web 12/16/2000

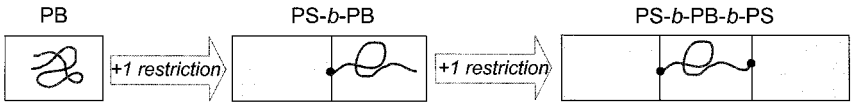

Figure 1. Schematic representation of the polymer systems used in this study. PB is a low-T_g material with extensive molecular motion at ambient temperature. In PS-*b*-PB, one chain end is fixed, and therefore, chain dynamics are limited. In PS-*b*-PB-*b*-PS, both chain ends are fixed, leading to further restrictions for polymer motion.

Table 1. Characterization of the PS-*b*-PB Diblock Copolymers Used in This Study[a]

system	PS-*b*-PB 900−600	PS-*b*-PB 12K−10K	PS-*b*-PB 22K−24K	PS-*b*-PB 90K−120K
M_n(PS)	900	12 000	22 000	90 000
M_n(PB)	600	10 000	24 000	120 000
T_g(PS), °C		+84.6	+90.5	+100.0
T_g(PB), °C	−38.6[b]	−97.1	−96.4	−95.6
L_{exp}, nm		21	35	
L_{theo}, nm		19	31	85
Z	0	5	14	71

[a] The theoretical lamellar spacing, L_{theo}, was calculated from $L_{theo} = 0.024M_n^{2/3}$.[13] [b] Only one T_g is observed.

transition temperatures, T_g, are summarized in Table 1. Molecular weights were determined via a combination of size-exclusion chromatography (SEC) and solution-state proton NMR, whereas glass-transition temperature data were obtained from differential-scanning calorimetry (DSC). The system with the shortest blocks is not microphase separated and thus a lamellar spacing cannot be determined. As another result of a lack of block segregation, only one broad glass transition was observed by DSC. On time scales of milliseconds, though, NMR detects dynamic heterogeneity, and as was the case for all systems under investigation, only in the range of $T_g(PB) < T < T_g(PS)$ chain dynamics of the PB block were monitored. However, it should be noted that differences in the dynamic behavior of the diblock co-oligomer (PS-*b*-PB 900−600) observed in NMR is due to the incomplete microphase separation of the sample and thus of totally different origin. For our longest diblock copolymer, the lamellar spacing is too large for SAXS to detect it, yet TEM clearly indicated the existence of a lamellar morphology.

Since entanglements are expected to have a significant influence on local order[3,4] and main-chain dynamics,[7,8] the entanglement molecular weight of 1,4-PB, M_e(PB), will be introduced here. The number of entanglements per PB is given by

$$Z = \frac{N}{N_e} = \frac{k}{k_e} \quad (1)$$

where N is the overall degree of polymerization of the PB chain and N_e the number of butadiene units between two adjacent entanglements. In later discussions, the number of Kuhn segments per chain, k, will be used rather than N, since, if the polymer chain is theoretically described in terms of Kuhn segments, conformational changes along the chain resemble Gaussian statistics. In this picture, k_e represents the number of Kuhn segments between two adjacent entanglements. M_e(1,4-PB) has been found to be 1700.[14] We assume that this value is also a good approximation for the PB blocks.

As a system with two tethered PB chain ends, an industrial PS-*b*-PB-*b*-PS triblock copolymer named RCM1 was investigated, which was provided by BASF AG, Ludwigshafen, Germany. The material usually serves as a compatibilizer to improve mechanical properties of recycled polymer blends. RCM1 represents a symmetric triblock copolymer of narrow molecular-weight distribution with two PS blocks of approximately 30 000 and a PB block of 20 000 (PS calibration) and exhibits two glass transitions at $T_g(PS) = +74.4$ °C and $T_g(PB) = -99.4$ °C. RCM1 displays a hexagonal morphology where PB cylinders are distributed in a continuous PS matrix. The polydispersity of all studied materials was below $M_w/M_n = 1.1$.

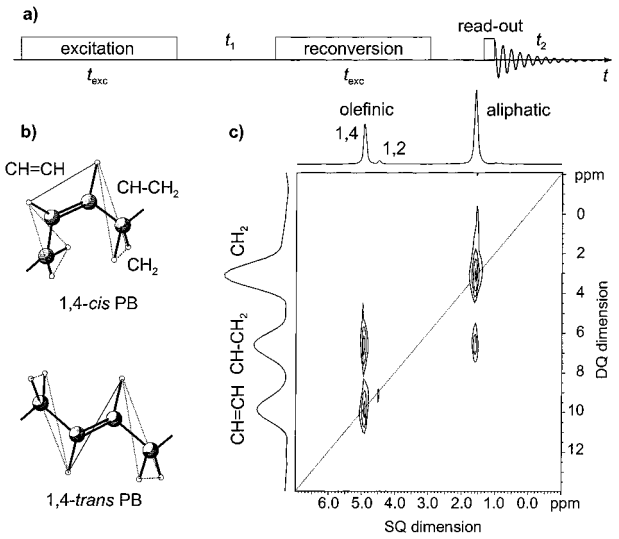

Figure 2. (a) Schematic representation of a DQ-NMR experiment. (b) Dipolar couplings present in *trans*- and *cis*-1,4-repeat units of PB in a PS-*b*-PB 22K−24K diblock copolymer that give rise to different DQ coherences and (c) the resulting two-dimensional ^{1}H DQ-NMR spectrum at 298 K and a Larmor frequency of 500 MHz. MAS spinning frequency was 6.8 kHz and the excitation time 0.8 ms. Note the trace of 1,2-PB at 4.7 ppm. Because of different chemical shifts, separate evaluation of 1,4-PB is possible.

2.2. DQ-NMR Spectroscopy. Double-quantum (DQ) NMR under fast magic-angle spinning (MAS) is a new tool to study structure[15,16] and dynamics[5,6] of polymeric materials. In solid-state MAS NMR DQ coherences can be excited by high-power radio frequency (rf) pulses utilizing the effective dipolar coupling. Typically, DQ coherences are observed in the first dimension (ω_1) of a two-dimensional NMR experiment, as depicted in Figure 2a. The rf-pulse train incorporates a DQ excitation part, a delay time, t_1, which is incremented for 2D experiments and constant ($t_1 = 0$) for DQ-filtered spectra, a reconversion part and a final read-out pulse prior to detection. Under fast MAS the DQ excitation and reconversion is achieved by appropriate recoupling techniques based on rotor-synchronized rf-pulse irradiation. To obtain experimental results comparable to earlier experiments in homogeneous PB melts[5] and SBR elastomers,[6] Levitt's C7 pulse sequence[17] was used for DQ excitation and reconversion. A typical two-dimensional DQ NMR spectrum for a PS-*b*-PB diblock copolymer is shown in Figure 2c. Since the experimental temperature is chosen between the glass transitions of the PS and PB block, the dipolar couplings between the ^{1}H nuclear spins of the styrene units are close to their static values. During the elaborate excitation/reconversion process of the applied recoupling sequence the DQ magnetization for styrene proton pairs is completely relaxed before the read-out pulse is irradiated and thus no DQ signals stemming from the PS block are detected. A series of two-dimensional DQ spectra was used to analyze the DQ excitation behavior of the different proton pairs in the butadiene units,[5] whereas the temperature-dependent spectra were recorded as one-dimensional DQ-filtered experiments with an excitation time of 0.8 ms. To obtain absolute values of the DQ intensity and to compensate for relaxation effects under the recoupling pulse sequence and for temperature dependences of the NMR probe, the measured DQ intensity is compared to a reference experiment under the

same conditions, where the DQ selection during t_1 is skipped and hence all excited coherences are reconverted into longitudinal magnetization. It should be mentioned that first-order phase errors occurring for long recoupling times in the t_1-dimension affect the signal intensities of DQ-filtered measurements, which however can be compensated for in the full 2D DQ NMR spectrum. All NMR experiments were performed on a Bruker ASX spectrometer at a proton Larmor frequency of 500.13 MHz equipped with a commercial variable temperature double-resonance 4 mm MAS probe at a spinning speed of 6.8 kHz. With this probe the whole temperature range between T_g(PB) and T_g(PS) is accessible to MAS NMR experiments. It should be noted that the line widths of proton lines of PB as obtained by ^{1}H MAS NMR change markedly over this temperature range, see for instance refs 3 and 4. They reflect both relaxation due to segmental motions and residual dipole−dipole couplings; the extracted integrated intensities of the DQ signals, however, reflect the residual dipolar couplings only, while relaxation effects being taken into account in the fitting procedure of the intensities as a function of the excitation time.[6]

3. Correlating Theory and Experimental Data

3.1. Dynamic Order Parameters. Order parameters are probably best known from the vast field of liquid-crystal research, where they are a common means to describe a state of matter that incorporates both molecular dynamics and long-range order.[18] The key idea of the order parameter concept is the definition of a director, $\vec{n}$, which defines a preferred direction in a region of the sample. This renders molecular motion of all residues within that region anisotropic. For simplicity we will consider uniaxial systems only. Then, any direction within a residue will *on average* rotate about the director. The order parameter for direction i, S_i, is a measure of the deviation from perfect alignment along $\vec{n}$. Thus, in a uniaxial liquid-crystalline phase formed by a rodlike compound on average at any instant all molecular long-axes have the same preferred orientation (ensemble average, index n). Although each molecule fluctuates about the director, on average its long-axis also points in this direction (time average, index τ). The degree of uniaxial ordering is usually described in terms of the second Legendre polynomial

$$S_i = \frac{1}{2}\langle 3\cos^2\theta_i - 1\rangle_{n,\tau} \qquad (2)$$

where the brackets denote time and ensemble averaging and θ_i is the angle between the molecular direction and the director.[19,20] S has a value of 1 for perfect parallel alignment, $-1/2$ for perpendicular order, and 0 for the isotropic case. As liquid-crystalline phases are commonly observed for form-anisotropic residues such as rods or disks, it is customary to specify *the* order parameter, S, for the unique direction of such residues, e.g., the long axis of rods or the normal to disks.

Finite order parameters are also predicted for chain segments between cross-links in polymer networks or topological constraints in melts, even if they do not incorporate any structural elements of extended geometrical anisotropy.[21,22] Yet in contrast to liquid-crystalline phases where long-range order exists on a range of a few micrometers and can be macroscopically aligned, the ensemble average for the whole polymer network is isotropic as long as the sample is not stretched. But still, on a microscopic level, e.g., in the principal axis system of each individual Kuhn segment which is affected by cross-links as shown in Figure 3, the time

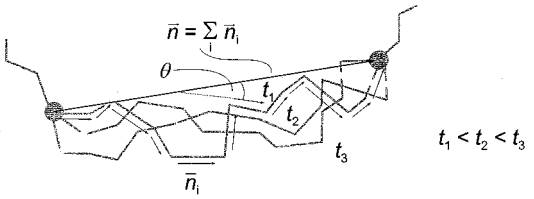

Figure 3. Time-dependent variation of the chain conformation for a polymer segment being constrained to invariant cross-links. Each unit i between two cross-links points on average in a unique direction giving rise to a dynamic order parameter. The constraints entanglements impose are projected on effective cross-links depicted as solid circles.

average is not isotropic. The local order parameter in polymer melts experienced by a given repeat unit can be defined for times longer than typical local reorientations and shorter than large scale translational motions. In this time regime, the corresponding mesoscopic ordering is described by a dynamic order parameter, S, given by

$$S_i = \frac{1}{2}\langle 3\cos^2\theta(t) - 1\rangle \qquad (3)$$

where θ now describes the angle between a local chain axis and the director imposed by surrounding chains. The dynamic order parameter, S, for a chain segment clamped between two cross-links is correlated with the director $\vec{n}$ that connects these structural constraints.

Chains can take up different conformations, but on average, they are oriented parallel to the director that connects the two adjacent cross-links or entanglements. The lower limit for the value of the dynamic order parameter of a polymer chain between two spatially fixed points depends only on its number of Kuhn segments, k_e, between them[21] according to

$$S_i = \frac{3}{5}k_e^{-1} \qquad (4)$$

Any further motional processes like slow dynamics of the "fix points" result in an additional reduction of the order parameter. Systems without any structural constraints will eventually behave isotropically on long experimental time scales. These considerations hold not only for chemical networks but also for entangled systems on the time scales on which entanglements act as physical cross-links. Structural relaxation such as the overall translational motion of the center of mass of a molten polymer chain also causes an additional reduction of the local dynamic order parameter because a given repeat unit experiences different ordered regions in the melt. There is ample evidence that segmental motion and displacements over the distance between entanglements occur on different time scales.[8]

Previous experimental approaches seemed to confirm the theoretical prediction of ordering for chain segments in chemical or physical polymer networks according to eq 4.[22−27] For instance, solid-echo NMR methods were used to determine order parameters experimentally. Pioneering work along this line was carried out by Cohen-Addad who studied dipolar interactions in entangled 1,4-*cis*-PB melts and found $S \approx 0.003$.[22] Collignon et al. investigated protonated and deuterated polyethylene melts and determined order parameters of 0.02.[24] Valic et al. found order parameters of 0.001 for a deuterated PB probe (with $M < M_e$) mixed in a

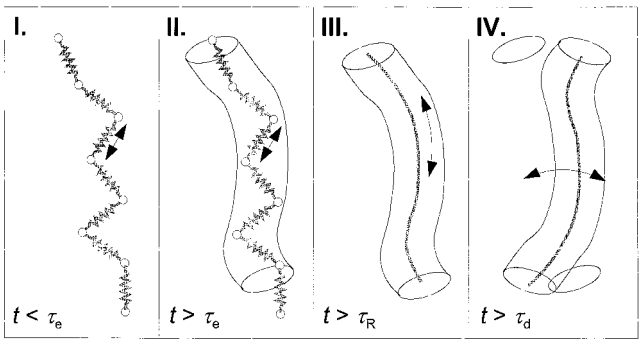

Figure 4. Illustration of the dynamic regimes which are predicted by de Gennes' reptation model. With each regime a particular scaling law is associated.

PS-*b*-PB matrix.[25] Monitoring dipolar couplings between protons in PDMS melts Ball et al. yielded order parameters of about 0.01.[23] Callaghan et al. applied similar methods on natural rubber (cross-linked 1,4-*cis*-PI) and determined $S \approx 0.01$.[26,27]

Little attention, however, was paid so far to the fact that measured order parameters can reflect different kinds of motions, e.g., segmental motions and backbone fluctuations. Recently, we developed a novel approach involving DQ MAS NMR that is capable of distinguishing between the different proton−proton dipolar couplings present in a repeat unit of PB and thus allows us to analyze corresponding order parameters separately.[5,6] For the proton frame within a repeat unit of 1,4-PB, three unique axes and correspondingly also three different order parameters, $S_{CH=CH}$, S_{CH-CH_2}, and S_{CH_2}, can be distinguished. Note that the directions probed by $S_{CH=CH}$ and S_{CH-CH_2} point *along* the polymer backbone and thus allow a better measure of chain ordering than S_{CH_2}. We measured dynamic order parameters of the order of $S_{CH=CH} = 0.13$ for the olefinic protons in 1,4-PB melts at $T = T_g + 50$ K and order parameters of $S_{CH-CH_2} = 0.17$ and $S_{CH-CH_2} = 0.13$ for cross-linked SBR rubbers and their non-crosslinked analogues, respectively.[6,28] These values are at least 1 order of magnitude higher than those estimated by eq 4. This finding was attributed to packing effects.

3.2. The Reptation Model. The chain motion of entangled polymers in the melt is conveniently described within the framework of de Gennes' reptation model.[7,8] Like the Rouse model, which describes a polymer chain as an assembly of oscillating beads connected by springs on intermediate time and length scales and is valid for short polymers only,[29] the reptation model considers single chains, but in contrast to the Rouse model interactions with surrounding chains are included. In particular, in the reptation model one assumes that spatial restrictions due to entanglements can be described by an effective tube. De Gennes' model predicts the time dependence of the mean-square displacement in four different dynamical regimes each being characterized by distinct scaling laws (Figure 4). Correspondingly, three crossover times can be distinguished. The nomenclature for denoting the different time scales is not unique in the literature. Here, the definition of Doi and Edwards[8] is used. Regime I resembles Rouse dynamics of a single polymer chain, described by a bead/spring model. It is characterized by short range conformational fluctuations which are represented by Rouse modes in which individual segments experience their connectivities to adjacent polymer segments, but interactions with surrounding chains are neglected. The characteristic scaling law of the mean-square displacement is $\sim t^{1/2}$. Exceeding a characteristic time, τ_e, the regarded chain starts to experience the effect of entanglements created by neighboring chains. Hence, regime II is a characteristic result of the reptation model. Although in this regime the considered chain is still carrying out Rouse-like dynamics, the motions are more anisotropic in comparison to the simple Rouse model due to the restrictions imposed by the spatial constraints of the surrounding chains. As the characteristic scaling law for the translational mean-square displacement a $\sim t^{1/4}$ dependence is predicted. On an even longer time scale, above its Rouse time, τ_R, in regime III, the regarded polymer chain starts to carry out a one-dimensional diffusional process along its contour inside the reptation tube in a curvilinear way. In this regime the chain is said to reptate; i.e., it creeps in a similar fashion as a snake does. The corresponding scaling law is predicted to be $\sim t^{1/2}$. Finally, at $t > \tau_d$, in regime IV the tube reorganizes, and chain motion becomes isotropic. In this regime, the scaling law is $\sim t^{1}$ as known from isotropic diffusion. In addition to predicting the scaling laws for the various dynamical regimes, the reptation models allows one to determine characteristic times, τ_i, also. The characteristic time above which the influence of entanglements becomes important is expressed as

$$\tau_e \approx \frac{\zeta(T) k_e^2 b^2}{\pi k_B T} \tag{5}$$

To estimate τ_e the friction coefficient, $\zeta(T)$, can be obtained from the Vogel Fulcher expression

$$\zeta(T) = \zeta_0 \exp\left(\frac{1}{\alpha(T - T_{VF})}\right) \tag{6}$$

where $\zeta_0 = 1.26 \times 10^{-14}$ N s m^{-1}, $\alpha = 7.12 \times 10^{-4}$ K^{-1} and $T_{VF} = T_g - 50$ K.[21,30] The necessary data on the systems are summarized in Table 1. Kuhn's segment, *b*, for 1,4-*cis*-PB and 1,4-*trans*-PB is estimated according to

$$b = 0.45 C_\infty^{cis} l^{cis} + 0.55 C_\infty^{trans} l^{trans} \tag{7}$$

where the values of C_∞, 4.7 for the cis and 5.8 for the trans species, can be found in the literature for homo-PB.[31] The numerical prefactors account for the distribution of cis and trans units in the chains revealed by solution-state proton NMR, and $l^{cis} = 4.4$ Å and $l^{trans} = 5.1$ Å follow from geometrical considerations. For calculating the time scale for the diblock copolymers we applied the same parameters (C_∞, k_e, ζ_0, α) as for homo-PB but took into account slight variations in the glass-transition temperatures in T_{VF}. Furthermore, k_e in eq 5 characterizes the distance between two entanglements in terms of Kuhn segments. In many relations the number of entanglements per chain, k/k_e, as introduced in eq 1 appears. For the sake of clarity, this quantity will be taken as *Z* later on. Of all the characteristic crossover times discussed here, only τ_e is independent of the size of the polymer chain and can therefore be used to normalize the time axis when dynamics of polymers with varying molecular weight are to be compared.[5] The equation describing τ_R is of the same form as resulting from the Rouse model but is here given in terms of τ_e and reads

$$\tau_R = \frac{Z^2}{3}\tau_e \tag{8}$$

At τ_d, chain motion becomes isotropic, and thus this time is termed the disengagement time. It is also known as the terminal relaxation time in mechanical measurements[21] and is given by

$$\tau_d \approx Z^3\tau_e \tag{9}$$

Thus, τ_d is most strongly dependent on the chain length. The reptation model was the subject of numerous theoretical[32−35] as well as experimental investigations[36−43] and although being still debated experimental evidence was obtained that supports this model. Besides de Gennes' reptation model, which is admittedly simple to visualize, there is an alternative theoretical model that is capable of describing several phenomena related to polymer dynamics: the mode-coupling theory, an approach that involves a continuum of relaxation times and takes a nonlinear coupling of collective density fluctuations of the surrounding chains and segmental density fields of the regarded chain on the length scale of R_g into account, predicts the molar-mass dependence of the self-diffusion coefficient, shear viscosity, longest relaxation time, and plateau modulus just as well as the tube model.[44−46] Moreover, scaling laws for the intermediate regime, $\sim t^{9/32}$ for Rouse-like motion inside the tube and $\sim t^{9/16}$ for center of mass motion, turn out to be very close to the $\sim t^{1/4}$ and $\sim t^{1/2}$ behavior in de Gennes' terminology. The mode-coupling theory was also applied to study self-diffusion in diblock copolymers.[47]

3.3. The DQ-NMR Technique. The dipolar interaction between protons is a particularly useful means to study the dynamics of polymeric systems since molecular motions have an averaging effect on the magnitude of the dipolar coupling.[48] Hence, its strength has to be described by motional averages $\langle D_{ij}\rangle$ rather then the static coupling constant D_{ij}. The advantage of investigating protons is 2-fold: high NMR sensitivity given by a large magnetogyric ratio and their ubiquitous appearance in organic macromolecules along with high natural abundance make protons suitable probes for investigating polymer dynamics. An elegant way to measure dipolar couplings is the DQ MAS NMR technique,[15] because only pairs of nuclear spins with finite dipolar coupling contribute to spectral intensity. Hence, the intensity of a DQ coherence directly reflects the strength of the dipolar coupling. In the following, the formalism that governs the relation between D_{ij} and the DQ intensity will be presented (see also refs 6 and 15).

The DQ intensity, I_{DQ}, can be written as a function of the excitation time, t_{exc}, and the reconversion time, t_{rec}, (Figure 2a) according to

$$I_{DQ} = \int_0^{t_{exc}} dt' \int_{t_{exc}+t_1}^{2t_{exc}+t_1} dt'' \,\langle \sin(\omega_{ij,eff}(t') \times t') \times \sin(\omega_{ij,eff}(t'') \times t'')\rangle \tag{10}$$

where $\omega_{ij,eff}$ depends on the excitation efficiency of the recoupling sequence as well as on the orientation of the corresponding molecule. The quantities t' and t'' are times within the excitation and reconversion periods, respectively. As long as the argument of the sine terms is small enough (short excitation times and weak dipolar couplings), eq 10 can be simplified by using only the arguments and substituting the time averaging brackets by integrals to yield

$$I_{DQ} \approx \int_0^{t_{exc}} dt' \int_{t_{exc}+t_1}^{2t_{exc}+t_1} dt'' \,\langle \omega_{ij,eff}(t')\omega_{ij,eff}(t'')\rangle \tag{11}$$

where t_1 is the time increment for two-dimensional experiments and is zero in the case of one-dimensional DQ-filtered experiments. This integral can be further simplified, if the sample is either rigid or if the correlation time, τ_c, of a dynamic process is much shorter than the experimental time scales t_{exc} and thus the dynamic effect can be taken into account via a pre-averaged, residual dipolar coupling $D_{ij,eff} = S_{ij}D_{ij}$. Since the residual dipolar coupling is assumed to be constant on the experimental time scale, the time dependence in eq 11 vanishes in both cases and the equation transforms to

$$I_{DQ} = \bar{F}_{DQ}{}^2\, D_{ij,eff}{}^2\, t_{exc}{}^2 = \bar{F}_{DQ}{}^2\, D_{ij}{}^2\, S_{ij}{}^2\, t_{exc}{}^2 \tag{12}$$

Equation 12 holds for rapid segmental motions of the first dynamic regime of the reptation model and leads to a preaveraging of the static dipolar coupling D_{ij}. It, therefore, predicts an initial plateau value in $I_{DQ}(t)$ depending on the local order parameter S_{ij}. However, the separation on logarithmic scales of the correlation times for different dynamic processes described by the reptation model is needed for eq 12 to be applicable. For the intermediate dynamic regime, $\tau_c \approx t_{exc}$, which includes the second and third motional regimes of the reptation model, the molecular dynamics during the DQ excitation and thus the time dependence of eq 11 has to be taken into account via an extra correlation term $C_R(t_{exc} + t_1)$. This correlation term reflects the angular dependence of the DQ excitation scheme, and is for the applied C7 sequence of the form

$$C_R(t_{exc} + t_1) = 5\left\langle d^{(2)}_{2,-1}\left(\frac{1}{2}t_{exc}\right) d^{(2)}_{2,-1}\left(\frac{3}{2}t_{exc} + t_1\right)\right\rangle \tag{13}$$

where $d^{(2)}_{2,m}$ denotes elements of the second rank Wigner rotation matrix in the convention of Reference 49. Equation 11 finally reads

$$I_{DQ} = \bar{F}_{DQ}{}^2\, D_{ij}{}^2(r) t_{exc}{}^2 S_{ij}{}^2 C_R(t_{exc} + t_1) \tag{14}$$

$\bar{F}_{DQ}{}^2$ is a function that describes the recoupling sequence and is the average over the orientation-dependent numerical prefactors of the excitation efficiency. We have mentioned in a previous publication that the approximative evaluation of the integral given in eq 11 using a two-time correlation function to yield eq 12 holds very well for processes described by algebraic time dependences (as is of interest here) but breaks down for, e.g., exponential decays.[5] Strictly speaking, eq 14 can be derived only if the rapid and intermediate time scales are uncoupled and well separated on a logarithmic scale as given by the reptation model.

The correlation-loss-function, $C_R(t)$, contains information about the intermediate dynamic regime, and therefore, it can be expected that it exhibits scaling laws characteristic for distinct motional processes of structural relaxation. Let us now evaluate the exponents that are predicted for $\tau_e < t < \tau_R$ and $\tau_R < t < \tau_d$ according to the formalism given above and introduced for the reptation model earlier in section 3.2.

Evaluation of $C_R(t)$ is possible under the simplifying assumption that a segment keeps its original average orientation as long as it is in its location between two specific entanglements. Assuming in addition a perfectly stable tube, $C_R(t)$ can be understood as the return-to-origin probability for a chain segment.[23] Hence, those repeat units which have not left their initial location between two specific entanglements and those which returned after some excursions to their initial location are assumed to contribute equally to the DQ intensity, and others do not. Under these conditions, *C(t)* loses its explicit dependence on the index *m* of the Wigner matrix element $d^{(2)}_{2,m}$, since the correlation functions for isotropic motions only depend on the rank l of the interaction.[49] Thus, $d^{(2)}_{2,m}$ can effectively be replaced by the second-order Legendre polynomial P_2, see also ref 5. Similar to the formalism given in ref 23, it can be written as

$$C_R(t) = \int_{-a/2}^{+a/2} f(r,t)\, dr \qquad (15)$$

where a is the diameter of the tube and $f(r,t)$ is the Gaussian bell function

$$f(r,t) = \frac{1}{\sqrt{2\pi\sigma(t)^2}} \cdot \exp\left(-\frac{r^2}{2\sigma(t)^2}\right) \qquad (16)$$

with $\sigma(t)^2$ being the mean-square displacement. An involved formalism given in the appendix of Graf's thesis[50] combined with expressions of the reptation model yields

$$\pi \cdot \tau_e \le t \le \pi \cdot \tau_R:\ \sigma(t)^2 = \frac{2Za^2}{3\pi^{3/2}}\sqrt{\frac{t}{\tau_R}} \qquad (17)$$

and

$$\pi \cdot \tau_R \le t \le \pi \cdot \tau_d:\ \sigma(t)^2 = \frac{2Za^2}{3\pi^2}\frac{t}{\tau_R} \qquad (18)$$

After inserting eqs 17 or 18 in eq 16, scaling laws can be estimated in the limit of long polymer chains ($Z \gg 10$)

$$\pi\cdot\tau_e \le t \le \pi\cdot\tau_R:\quad C_R(t) \approx \sqrt{\frac{3\pi^{3/2}}{2Z}\frac{\tau_R}{t}} \sim t^{-1/4} \qquad (19)$$

and

$$\pi\cdot\tau_R \le t \le \pi\cdot\tau_d:\quad C_R(t) \approx \sqrt{\frac{3\pi^{2}}{2Z}\frac{\tau_R}{t}} \sim t^{-1/2} \qquad (20)$$

The latter two scaling laws were experimentally observed for homo-PB.[5]

The time dependence of the correlation function, $C_R(t)$, is shown in a schematic way in Figure 5. The typical result of a DQ-NMR experiment is depicted as solid black lines with the characteristic scaling laws for the second and third dynamic regime. The rapid regime is detected as a plateau, i.e., a starting point for the subsequent loss of the return-to-origin probability. The corresponding scaling law is given by a $\sim t^0$ dependence.

Indeed, the motional regimes II and III as well as the crossover between them have been observed experimentally for PB melts.[5] In contrast to other techniques, which focus on translational motion by monitoring the mean-square displacements, we probe local chain order and detect translational motion as a process which leads to a decay of order that a given repeat unit experiences. As the regimes I through III are found experimentally, however, the nanometer length scales over which the order extends can be deduced based on the reptation model and its relation to macroscopic phenomena such as the viscosity. Also note that slight changes in S_{ij} between t_{exc} and t_{rec} due to limited stability of the tube will only slightly reduce the DQ intensity, if the direction of the local order remains the same. If, however, also the direction of the local tube changes with time, the DQ intensity will be drastically reduced.

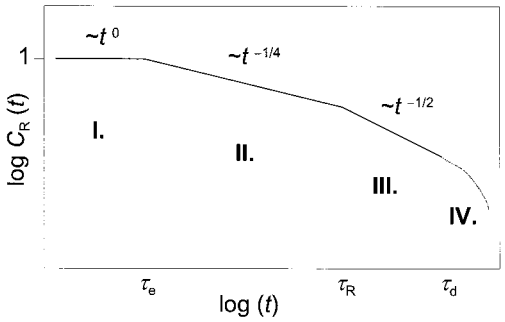

Figure 5. Visualization of the correlation function $C_R(t)$ in terms of the reptation model and a typical outcome of a DQ-NMR experiment that is able to probe this function. The black solid lines referring to regimes II and III are accessible by DQ NMR spectroscopy, whereas regime I is detected as a plateau value. Increasing temperatures or longer experimental time scales leads to a decrease of the residual chain portion in the original part of the tube at time t compared to time τ_R and to a decrease of the DQ intensity.

For polymer chains tethered to rigid objects, which is the case in heterogeneous diblock copolymers, a similar treatment is not yet available, since the mathematical relations are far more complex and, as a consequence, analytically not solvable. A short treatment on such systems, however, was provided by Graessley.[51] Nevertheless, on a qualitative level, one can easily rationalize that the dynamic regime III which incorporates the actual reptation motion process should not occur for mobile chains anchored to some rigid entity.

4. Results and Discussion

4.1. Dynamic Order Parameters. The reptation model predicts several different dynamic regimes for polymer motion, and an experimental way to monitor some of them has been presented above. The dynamic regime on the shortest time scale but still accessible by DQ NMR is characterized by rapid segmental motions with correlation times, $\tau_c < D_{ij}^{-1}$. This requires motions on time scales below 10 μs, which are typically reached at temperatures above T_g + 50 K. Then DQ NMR monitors preaveraged dipolar couplings that are constant over a considerable temperature range. For molten amorphous polymers, remarkably high chain order parameters were found. For the olefinic protons in 1,4-PB, averaged over the cis and trans configurations, this order parameter was observed to be as large as $S = 0.13$, indicating extensive local chain order on a time scale of milliseconds. The same value has been determined for non-cross-linked random styrene−butadiene copolymers, like PB another polymeric material of low functionality.[6] Even higher values were previously found for the carboxylic side groups in methacrylates: $S = 0.38$ for poly(methyl methacrylate) and $S = 0.70$ for poly-

Table 2. Plateau Values of the Residual Dipolar Couplings and Corresponding Dynamic Order Parameter Data for Various PS-*b*-PB Block Copolymers at T_g(PB) + 50 K[a]

		CH_2	$CH-CH_2$	CH=CH	C=C
rigid PB	$D_{ij,\,stat}$, kHz	21.0	6.1	7.0	
PB 130K[1]	$D_{ij,\,rel}$	1.00	0.43	0.75	
	$D_{ij,\,abs}$, kHz	1.2	0.5	0.9	
	S_{ij}	0.06	0.08	0.13	0.2
PS-*b*-PB 90K-120K	$D_{ij,\,rel}$	1.00	0.47	0.66	
	$D_{ij,abs}$, kHz	3.6	1.7	2.4	
	S_{ij}	0.17	0.28	0.34	0.56
PS-*b*-PB 12K-10K	$D_{ij,rel}$	1.00	0.59	0.63	
	$D_{ij,abs}$, kHz	3.8	2.2	2.4	
	S_{ij}	0.18	0.36	0.34	0.56
PS-*b*-PB-*b*-PS	$D_{ij,rel}$	1.00	0.62	0.93	
	$D_{ij,abs}$, kHz	4.4	1.7	2.9	
	S_{ij}	0.15	0.31	0.41	0.68

[a] For comparison, previously published data obtained for homo-PB are included in this chart.[5]

(ethyl methacrylate).[52] The ordering was attributed to the existence of entanglements[5] which form a physical network in high molecular-weight polymer melts. The preordering of chains in the melt is a highly cooperative phenomenon and is not significantly increased by introducing chemical cross-links as indicated by our results on random styrene-butadiene copolymers. A growing cross-link density was found to lead to enhanced local order, but the resulting order parameters do not exceed values of $S = 0.17$.[6,28]

The aim of the present work is to explore in which way rigid confinements affect local order. The confinements of polymer motion in the PB blocks are represented by rigid PS blocks, at $T < T_g$(PS), to which the PB chains are tethered on one end. In contrast to SBR where each chemical cross-link connects two polymer chains, in lamellar PS-*b*-PB diblock copolymers all PB chains over large domains are collectively fixed and all junction points are forced next to each other. Thus, the interface in a block copolymer is expected to impose much stronger topological constraints than chemical cross-links. Finally, a PS-*b*-PB-*b*-PS triblock copolymer will be examined in which also the second chain end is fixed.

In ^{1}H DQ MAS NMR, the dynamic order parameters are determined from DQ intensities, which are related to the dipolar couplings between two protons that give rise to the DQ coherence according to eqs 12 and 14. All three different dipolar couplings that are present in a butadiene repeat unit can be measured (Figure 2b). For the rapid dynamic regime, a constant DQ intensity is observed as a plateau or t^0 regime.[5] Since all three DQ intensities are measured in the same spectrum, the ratios between them are well-defined. Because the DQ intensity depends on experimental parameters, the determination of *absolute* values of the order parameter requires *absolute* measurements of at least a single residual dipolar coupling. In PB homopolymer melts, this was achieved by evaluating the ^{1}H MAS sideband intensity for the CH_2 protons in a single-quantum spectrum.[5] This approach is, unfortunately, not applicable for block copolymers due to significant susceptibility effects.[53] However, as the relation between DQ intensity and dipolar coupling constants for PB homopolymer melts is established via MAS sideband analysis[15] DQ intensity data can be analyzed to yield the respective dipolar coupling also for PS-*b*-PB block copolymers by comparing DQ data obtained for the

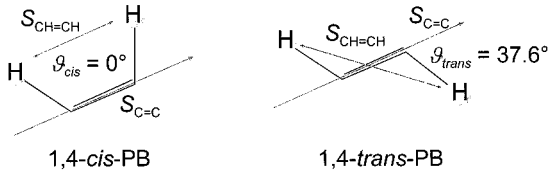

Figure 6. Correlating the dynamic order parameters $S_{CH=CH}(t)$ and $S_{C=C}(t)$ for cis and trans units in the PB block and angles ϑ_i used for the transformation of Legendre polynomials.[48]

homopolymer and the block copolymers recorded under the same experimental conditions. Note that $I_{DQ} \sim D^2$; thus, small differences in the spectrometer performance only slightly affect the determination of the residual order parameters. In DQ build-up curves for a PB 128K homopolymer we obtained relative dipolar couplings D_{CH_2}:D_{CH-CH_2}:$D_{CH=CH}$ = 1:0.43:0.75. According to external SQ MAS scaling experiments at 213 K, D_{CH_2} corresponds to 1.2 kHz. From this value a residual dipolar coupling of $D_{CH=CH} = 0.9$ kHz was calculated. In the diblock copolymers the DQ intensities are much higher, yielding $D_{CH=CH} = 2.4$ kHz. For PS-*b*-PB-*b*-PS triblock copolymers, the normalized DQ intensity for the olefinic proton interaction turns out to be even higher, resulting in a residual dipolar coupling constant $D_{CH=CH} = 2.9$ kHz. Through comparison with respective static values known for rigid systems, these plateau values of residual dipolar interaction can be related to order parameters according to

$$S_{ij}(t) = \frac{D_{ij,\mathrm{eff}}}{D_{ij,\mathrm{stat}}} \tag{21}$$

Corresponding values along with dipolar coupling raw data are summarized in Table 2 for a PB homopolymer, two PS-*b*-PB diblock copolymers, and a PS-*b*-PB-*b*-PS triblock copolymer where also the second PB chain end is anchored.

Proton DQ NMR experiments can distinguish three dynamic order parameters, $S_{CH=CH}(t)$, $S_{CH-CH_2}(t)$, and $S_{CH_2}(t)$. To describe the main-chain dynamics in a proper way, the dynamic order parameter of a direction along the polymer chain itself is desired. In the case of PB, the dynamic order parameter of the double bond between the two olefinic carbon atoms, $S_{C=C}(t)$, is expected to display the highest order parameter of the polymer chain, because the double bond acts as a stiffening element within each repeat unit. According to standard recipes,[18,48] a transformation of Legendre polynomials

$$S_{CH=CH}(t) = P_2(\cos\vartheta) \times S_{C=C}(t) \tag{22}$$

relates order parameters for different directions (Figure 6). We checked via simulations[5,54] that the relative ratios of the different experimentally observable order parameters are consistent with the rotational isomeric state (RIS) statistics[31] of the chain and, by trial and error, did not identify a direction within the butadiene unit which would display order parameters higher than directions along or close to the C=C double bond. It should be noted that $S_{CH=CH}$ data represent an average of the individual contributions of the cis and trans units, which, in contrast to homopolymers, cannot be resolved in the ^{1}H NMR experiments for PS-*b*-PB block copolymers. The average order parameters along the polymer chain for both the CH=CH and the C=C directions can

be determined from

$$S(t) = 0.55S_{trans}(t) + 0.45S_{cis}(t) \qquad (23)$$

where the weighing factors refer to the microstructure present in the PB chains as revealed by solution-state NMR. For PB homopolymers we found $S_{C=C,trans} \approx 2S_{C=C,cis}$ estimated indirectly from ^{1}H NMR according to eq 22.[5] Recent ^{1}H−^{13}C heteronuclear DQ NMR data show that this ratio also prevails in the block copolymers.[55]

This procedure yields remarkably high order parameters for the PB block in PS-*b*-PB diblock copolymers of $S_{C=C}(t) = 0.56$ as compared to 0.2 for homo-PB.[5] A particularly noteworthy result is the observation that the order parameters are the same for all diblock copolymers under investigation and, thus, do not depend on the chain length or the lamellar spacing. This implies that the effect that causes main-chain ordering must influence the entire mobile phase. Gradients in the order parameter would imply even higher values at the interface.

The order parameters for both, homo-PB and PS-*b*-PB diblock copolymers, are much larger in magnitude than is theoretically predicted by eq 4.[21] This leads us to the conclusion that substantial additional influence on local order must be based on interchain packing. As pointed out above the order parameter of trans units is determined to be twice as large as that of the cis units. This is in accord with findings that the packing for 1,4-*trans*-PB is much denser than for 1,4-*cis*-PB since chain alignment is hindered in the case of the somewhat bulkier cis units.[14,56]

When also the second PB chain end is anchored, a further increase of the C=C order parameter from 0.56 to 0.68 is observed. This is found for several different PS-*b*-PB-*b*-PS triblock copolymers. It should be mentioned that the dramatic increase in order parameters for PB in diblock and triblock copolymers is observed for *all* directions probed by ^{1}H DQ NMR. Differences in the ratios between the different directions are also found but the pattern remains similar.

4.2. Polymer Dynamics in Diblock Copolymers. The dynamics of PB on various time scales are now well understood and can be described within the framework of the reptation model.[5] On the basis of these results, the influence of further spatial constraints on the polymer dynamics of the mobile phase can be studied. In particular, it is of interest to examine the interplay of entanglements in the mobile phase and anchoring the highly mobile chains to a rigid entity. In a PS-*b*-PB diblock copolymer a PB chain is tethered to a wall, and therefore, the PS block acts as a physical cross-link to a given chain and its neighbors close to the interface. PS-*b*-PB diblock copolymers of four different molecular weights were studied. The individual block copolymers will be distinguished by the molecular weight of the respective blocks. PS-*b*-PB 900−600 is a short diblock copolymer with a nonentangled PB block. It is also important to note that this copolymer is not microphase separated. The other three systems incorporate entangled PB blocks and exhibit a lamellar morphology.

The combination of microphase separation and dynamic heterogeneity of $(T_g(PS) - T_g(PB)) > 150$ K leads to the unique properties that make PS-*b*-PB diblock copolymers particularly suitable for our purposes. It is known that immobilization of the rubbery component occurs in the interphase. In related PS-*b*-PI polymers, Stöppelmann et al.[57] determined an interphase thickness of 1 nm via deuteron NMR techniques. We carried out similar experiments on deuterated PB chains for the short, phase-separated PS-*b*-PB block-copolymer 12K−10K (Table 1) and found, in combination with DSC results, that a chain segment of at most 15−20 repeat units is immobilized in the interphase of our block copolymer.[58] In accord with this finding, the observed ^{1}H NMR signals of the mobile PB chains in one-dimensional MAS experiments were found to correspond to the volume fraction of the PB block. As a consequence, we feel safe to neglect the small immobilized fraction associated with the interphase. Experimental order parameters for different block copolymers as well as analogous homopolymers are plotted as a function of temperature in Figures 7a and 8a. First note that the order parameters decay on a logarithmic scale for the diblocks, indicating translational motion of the individual segments. Also note that the order parameter is always probed experimentally on the same time scale in the millisecond range where we excite and reconvert DQ coherences. Via eqs 5 and 6, the experimental temperature scale can be converted into a time scale of polymer dynamics by assuming that the time−temperature superposition principle[21] holds for the systems. This implies that for the motional processes investigated in this work, raising the temperature should lead to a similar result as increasing the experimental time scale. Although commonly applied in polymer science, it should be realized that this assumption enters in all the conclusions drawn later. Therefore, the experimental data in Figures 7 and 8 below are presented in two ways, i.e., as a function of temperature as measured (Figures 7a and 8a) and after conversion of the temperature scale into a time scale (Figures 7b and 8b). Should the time−temperature superposition principle later prove to be inadequate here, the original plots (Figures 7a and 8a) will remain valid. In particular, the absolute maximum values of the chain order parameters observed at temperatures around $T_g + 50$ K do not depend on this assumption, whereas the exact values of the scaling coefficients do.

As the quantities that describe the anisotropic chain motion best, residual dipolar couplings between olefinic protons, $D_{CH=CH}$, and corresponding dynamic order parameters, $S_{CH=CH}$, obtained from eq 21 are employed. To eliminate a molecular-weight dependence of the time scale calculated from the temperature dependence via the time−temperature superposition principle, data are normalized with respect to τ_e, the only characteristic time in the reptation model that is independent of the chain length. This procedure yields charts of the form $S_{CH=CH} = f(t/\tau_e)$ or $D_{CH=CH} = f(t/\tau_e)$, respectively (Figures 7b and 8b), where t is the experimental time scale (typically slightly below 1 ms) given by the DQ excitation and reconversion time. Plotting experimental data in a log−log representation provides characteristic slopes for the scaling laws referring to the different dynamic regimes outlined in Sections 3.2 and 3.3 (see also Figure 5).

Insight into details of the main-chain dynamics of the PB block in a PS-*b*-PB diblock copolymer of varying molecular weight can be retrieved from Figure 7b. The maximum order parameter manifests itself as the plateau value for short times. It is the same for all molecular weights under investigation. As already mentioned, this implies that the chain order is not due

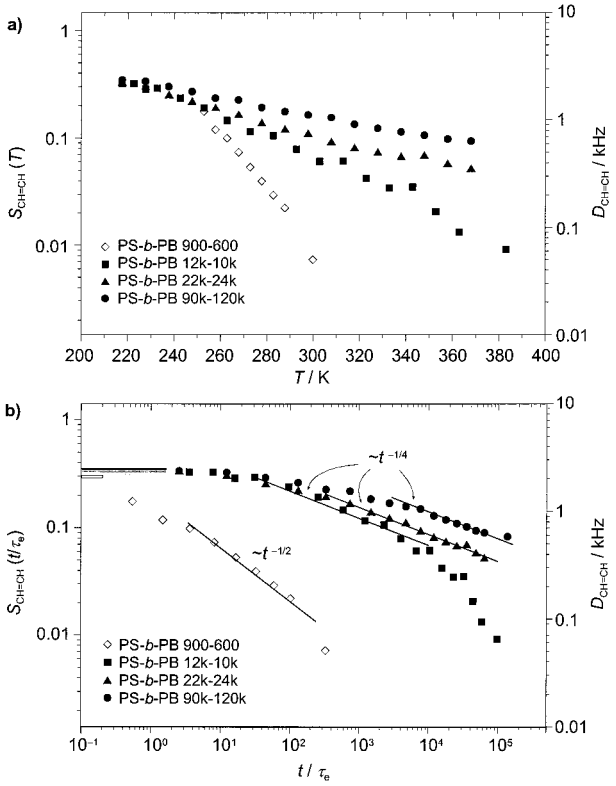

Figure 7. Temperature and time dependence of the intensity of the olefinic DQ coherence for a series of lamellar PS-*b*-PB diblock copolymers of varying molecular weight. Data are given as a function of (a) experimental temperature and (b) time after having converted the abscissa employing time−temperature superposition.

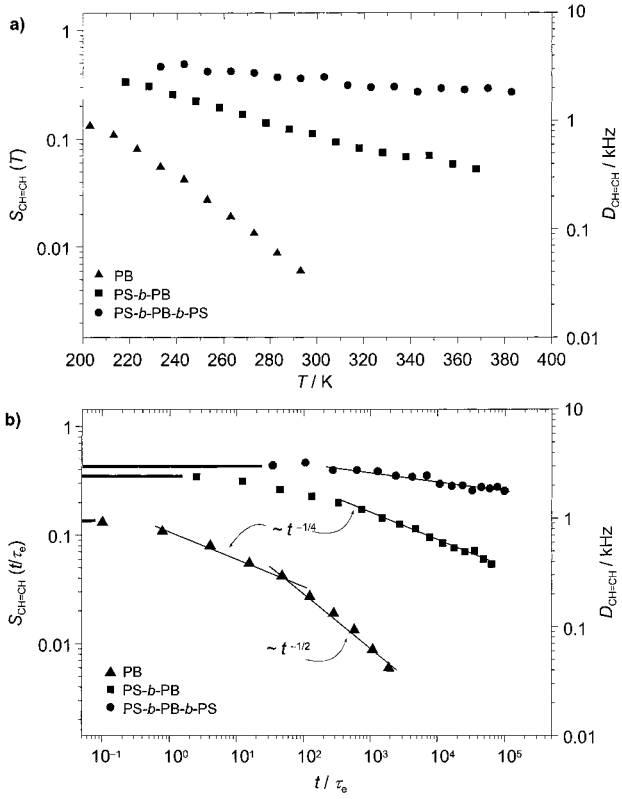

Figure 8. Effect of rigid confinements on local order and main-chain dynamics as observed by proton double-quantum NMR. Data are given as a function of (a) experimental temperature and (b) time after having converted the abscissa employing time−temperature superposition.

to highly organized chains of the structural interphase in the vicinity of the PS/PB junction points in the block copolymer but rather an ensemble effect of the complete PB block. At considerably longer times the systems enter the intermediate dynamic regime, where Rouse-like motion inside the reptation tubes with $\sim t^{-1/4}$ dependence takes place. For the three longer blocks that are above the entanglement molecular weight of the PB block, the dynamic regime which indicates the actual reptation of the chain through a $\sim t^{-1/2}$ scaling law is not observed. Instead, an extended $\sim t^{-1/4}$ regime is found. This can be interpreted as indicating that the tube is stabilized and Rouse-like dynamics occur on a longer time scale, but switching to diffusive reptation motion is restricted on account of the impenetrable nature of the PS block. For PS-*b*-PB 12K−10K an additional dynamic regime is observed at long time scales with a decay faster than $\sim t^{-1/2}$. This process might be due to an arm-retraction process. It is known that arm-retraction is suppressed for higher molecular-weight systems[51] and indeed this dynamic regime is not found for PS-*b*-PB 22K−24K or 90K−120K.

The short PS-*b*-PB 900−600 should not be subject to reptation dynamics because no entanglements are present. Nevertheless, the PB chains are also tethered and apparently are highly ordered for short times. The decay of the order parameter follows roughly a scaling law with $\sim t^{-1/2}$, which might be attributed to simple Rouse motion. For the entangled systems it is interesting to recognize the shift of the $\sim t^{-1/4}$ regime to longer time scales with increasing molecular weight. This has also been found for PB homopolymers[5] and semidilute PS solutions[42] and suggests a broadening of the cross-over from rapid segmental motions to tube-restricted Rouse motions. Theoretical computations on this cross-over region predict a molecular-weight-dependent broadening of the transition from a rapid to an intermediate dynamic regime.[59]

These findings are corroborated when the range of anisotropic polymer motion as obtained from DQ-NMR experiments is compared for PB homopolymers and the block copolymers (Figure 8). First, the marked increase of the maximum order parameter (plateau value) by tethering the chains should again be pointed out. Furthermore, the onset of the $\sim t^{-1/4}$-regime is shifted by about two decades in time for the block copolymers as compared to the homopolymer. These two observations taken together mean that chain order in a block copolymer is significantly increased and stabilized in the sense that a given repeat unit has a much higher return-to-origin probability in a block copolymer than in a homopolymer of the same molecular weight.

For data evaluation we used the same C_∞ parameters and k_e in eq 5 for all materials alike. Let us now examine to what extend the observed shift of the onset of regime II can be attributed to a mismatch of these estimated values. Feigin and Napper demonstrated that even an inert interface leads to a modification of conformational statistics and as a result the value of C_∞ for the tethered block is predicted to be $^4/_3$ of the homopolymer value.[60] For microphase-separated diblock copolymers Kremer and co-workers found in simulations that entanglement effects are reduced in the tethered molten block,[61] i.e., k_e in the block should be larger than in the homopolymer. Adjusting C_∞ and k_e causes a shift of our $S_{CH=CH}(t/\tau_e)$ curves. Since a value for C_∞ for the

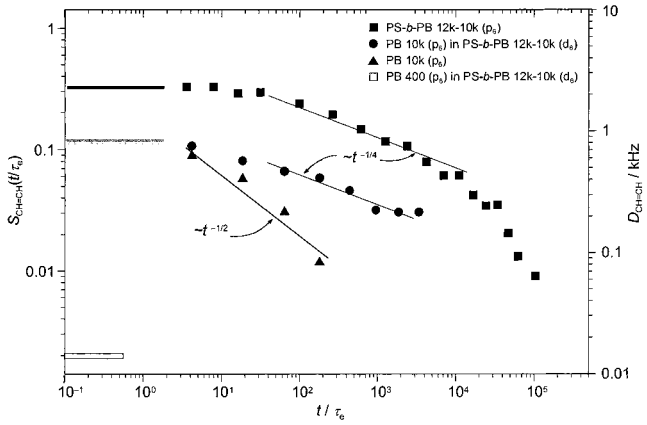

Figure 9. Dynamic order parameter of the olefinic coherence as a function of time for a PB of 10K molecular weight fixed to a PS block, a nonmodified PB 10K and a PB 10K that was mixed into a PS-*b*-PB 12K−10K with a perdeuterated PB block to obtain a 5% blend with respect to PB. Comparison of these systems allows one to get insight about the stability of a tube formed by entanglements.

block copolymer case is known[60] we are left with k_e as the only parameter that can be used to match the block copolymer and homopolymer curves. From this we estimate the effective k_e for tethered polymer chains in PS-*b*-PB 22K−24K (compared to PB 20K, Figure 8) to be k_e(PB block) $\approx 5k_e$(homo-PB).

Figure 8 also includes data on the main-chain dynamics of the triblock copolymer. Obviously, the PB chains are very effectively confined in such a system and the entire experimental time scale is governed by a $\sim t^0$ regime. In fact, this observation supports another assumption that we have tacitly used throughout, namely that the maximum order parameter does not decay on a logarithmic scale with increasing temperature. The slight decrease by about 30% observed in the triblock copolymer over a temperature range of more than 150 K does not alter our previous conclusions on translational chain motion being the major cause for the decay of the order parameter. Note that the correlation time of segmental dynamics changes by about 7 orders of magnitude over this temperature range.

4.3. Chain Order and Dynamics of Oligomers Dissolved in a Block Copolymer. To further elucidate the interplay of chain anchoring and entanglements we also studied whether the translational dynamics of a free chain is altered, if it is dissolved in a block copolymer. In Figure 9 the time dependence of the dynamic order parameter of the olefinic DQ coherence, $S_{CH=CH}$, for PB 10K and PS-*b*-PB 12K−10K are compared to that of a blend of 5 wt % PB 10K in a PS-*b*-PB 12K−10K block copolymer with a perdeuterated PB block. A schematic representation the structures of these three systems is depicted in Figure 10. The mixture of PB (p_6) 10K and PS-*b*-PB (d_6) 12K−10K allows one to investigate the translational motion of a PB chain in tubes that are created by entanglements of the PB block of the copolymer. Since the PB block of the copolymer is deuterated and proton NMR is performed, the experiment is exclusively sensitive on the dynamics of the protonated PB 10K probe. The low fraction of PB probes can be expected not to perturb any unique local chain ordering of the PS-*b*-PB matrix. Therefore, microscopic chain conformations and packing can be assumed to resemble those present in pure PS-*b*-PB. As an interesting result, the plateau order parameter of the PB probe mixed into the block copolymer matrix resembles that for the pure homopolymer. Strictly speaking, we have no rational explanation for finding exactly the same value. It is known from binary liquid-crystalline blends that the order parameter of a solute in a highly ordered matrix does not necessarily resemble the order parameter of the matrix but, depending on an interaction parameter, should rather lie between the values of the pure components.[18] Slight differences that fall within the experimental uncertainty cannot be resolved for these system.

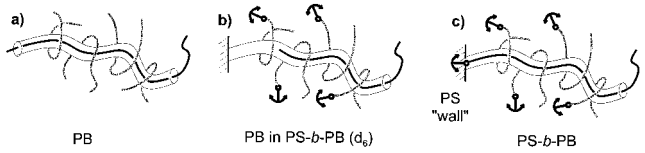

Figure 10. Schematic representation of PB in different surroundings: (a) where PB can reptate in an environment of the same material; (b) where PB can reptate in a tube formed by entangled chains of a PB block in a PS-*b*-PB block copolymer; (c) where PB is observed as an anchored block of a PS-*b*-PB block copolymer. Because of the fix point, the PB chain cannot undergo the actual reptation process. The anchors denote that the respective PB chain end is attached to a rigid PS "wall".

For the intermediate time scale the experimental curve found for the PB/PS-*b*-PB blend resembles the behavior typically observed for block copolymers and thus clearly exhibits the enhanced stability of the tube created by entangled chains in the PB block of the block copolymer in yielding a $\sim t^{-1/4}$ law. Although for this system appearance of a $\sim t^{-1/2}$ behavior is of course expected at longer times, the experimental signal-to-noise ratio prevents observation of this regime. Reptation motion of a homopolymer probe inside rigid tubelike channels was, however, observed by Fischer et al.[39] In contrast to the blend, the pure homo-PB is governed by a $\sim t^{-1/2}$ law as PB 10K is only slightly entangled. In a homopolymer, this small number of entanglements is too low for reptation motion to become prominent. In the block copolymer, however, disentanglement of chains is reduced since each PB chain that creates a topological constraint is itself tethered and thus restricted in its motional behavior. Translational motion apparently depends on the temporal stability of the tube.

To prove the importance of entanglements for the arguments outlined here, DQ NMR experiments were also performed on another mixture, namely of a PB (p_6) 400 homopolymer in PS-*b*-PB (d_6) 12K−10K diblock copolymer, where the PB probe is much shorter than the entanglement molecular weight. The plateau order parameter for this system was estimated to be $S_{CH=CH} \approx 0.002$, and no further dynamic regimes are found, clearly indicating that this homopolymer probe is too small for the mesh size of the entanglement-based physical network. This finding agrees with results published by Valic et al.[25]

4.4. Structural Implications of the Observed Chain Order Parameters. Our detailed study of chain order parameters observed at short times and their decay as a result of translational motion at longer times now allows us to propose a scenario of structure in amorphous polymers, as illustrated in Figure 11. From the scaling laws observed, we are forced to conclude that the ordering of chains occurs in regions with sizes governed by the entanglement molecular weight, i.e., a few nanometers. Hence, we call these regions nano-

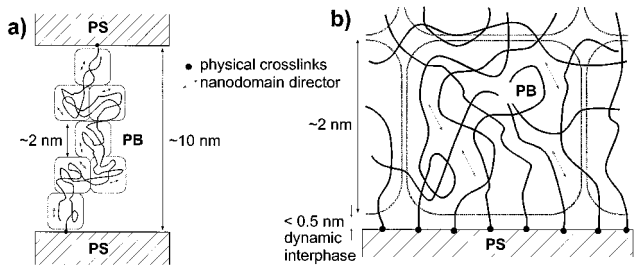

Figure 11. Rationalization of the typical length scale for local ordering in the flexible PB block in a PS-*b*-PB diblock copolymer with lamellar morphology (the case for PS-*b*-PB 22K−24K is depicted). PS/PB junction points are denoted by solid black circles and represent stable physical cross-links. The domains that exhibit chain ordering on short time scales are of the order of 2 nm. (a) One whole lamella and (b) an expanded view of a single nanodomain are depicted.

domains. In a homopolymer melt, the chains will reptate through those nanodomains, which are statistically independent. Therefore, the order parameter will decay essentially to zero. The fact that the order parameter decays on a logarithmic scale even in block copolymers implies that these nanodomains have different director orientations in block copolymers also (Figure 11a). The increase in order parameters in block copolymers as compared to homopolymers is rationalized in Figure 11b. As adjacent chains in the nanodomains close to the interface are preferentially aligned perpendicular to the rigid block, the collective chain order increases for the entire domain. Another way of looking at this is to realize that not single chains, but the nanodomains, are confined in the lamellae of the block copolymers, which themselves have a thickness of several nanometers.

We hurry to point out that our present findings cannot yet prove this scenario in all details, or beyond any doubt. Yet, it is consistent with all the observations, including those of mixing short chains in systems with longer chains. At any rate, dynamic chain order parameters emerge as a new means to characterize polymer chains in amorphous systems on the nanometer scale.

Furthermore, our results on chain ordering in polymer melts are in good agreement with recent findings by Strobl et al.[62] After intensive investigation of various semicrystalline polymers, including syndio- and isotactic polypropylene, polyethylene (with or without octene co-units) and poly-ϵ-caprolactone, using SAXS,[63] DSC, and AFM[64] as experimental techniques, Strobl and co-workers gathered data that allowed them to propose a new model for the polymer crystallization from the melt. In particular, they suggest that the actual crystallization follows a two-step mechanism involving a phase of nanometer-sized domains of preordered molten polymer chains referred to as granular crystalline phase. This novel phase is characterized by decreased chain dynamics, i.e., considerably ordered chains, and a cooperative structural phase transition is anticipated if the temperature is lowered to either form crystallites or raised to cause a complete melting. For our amorphous systems, crystallization is ruled out due to structural imperfections on a microscopic level, yet the tendency of preordering can be clearly seen.

In a forthcoming publication, where we studied the crystallization behavior of constrained semicrystalline poly(dimethylsiloxane) (PDMS), we observed that the crystallization rate is increased as a result from preordering of chains in the melt. We compared various physically or chemically cross-linked systems to their non-crosslinked analogues and found a higher tendency toward crystallization for all confined materials.[65]

5. Summary

The main-chain order and dynamics of the mobile PB block of several PS/PB block copolymers with one (PS-*b*-PB diblock copolymers) or two (PS-*b*-PB-*b*-PS triblock copolymers) terminal fix points per PB chain were investigated by high-resolution proton double-quantum MAS NMR. Individual motional regimes and how they are affected by rigid constraints were examined in detail. It was found that tethering PB chains to rigid objects has an influence on the entire PB block rather than on a small fraction in the vicinity of the interface only.

From previous studies on homopolymers, entanglements are expected to give rise to local dynamic order of the main chain. Corresponding order parameters for 1,4-PB were determined to be as large as $S_{C=C} = 0.2$ on a time scale of about a millisecond.[5] Introduction of rigid constraints in form of glassy PS blocks have now been found to result in an enhancement of local order with order parameters of $S_{C=C} = 0.56$ and $S_{C=C} = 0.68$ for the PB block in PS-*b*-PB diblock copolymers and PS-*b*-PB-*b*-PS triblock copolymers, respectively. These findings are attributed to stabilization of entanglements and, consequently, extended preordering of chains in the melt. The characteristic length scale of ordered domains is governed by the entanglement spacing, i.e., a few nanometers.

In terms of the reptation model, stabilization of entanglements by tethering one PB chain end was experimentally observed to lead to an extended second motional regime which involves Rouse-like dynamics inside the tube indicated by a characteristic $\sim t^{-1/4}$ scaling law. On account of anchored chain ends, the actual reptation motion in the third dynamic regime with a $\sim t^{-1/2}$ scaling law is lost for diblock copolymers as well as systems with two fixed chain ends.

Acknowledgment. Encouraging discussions with Profs. Sir Sam Edwards and Pierre-Gilles De Gennes are gratefully acknowledged. We would like to express our gratitude to Ralph Ulrich for performing SAXS measurements, Diane Babski for taking TEM micrographs, Uta Pawelzik for running the DSC experiments, and Sandra Seywald for SEC elugrams. We appreciate the cooperation with Stefan Lehmann of BASF AG, Ludwigshafen, Germany, who provided the triblock copolymer. The present study was funded by the Deutsche Forschungsgemeinschaft and was part of the Sonderforschungsbereich 262.

References and Notes

(1) Hamley, I. W.; *The Physics of Block Copolymers*, Oxford University Press: Oxford, England, 1998.
(2) Holden, G., Legge, N. R., Quirk, R. P., Schroeder, H. E., Eds.; *Thermoplastic Elastomers*, 2nd ed.; C. Hanser Verlag: Munich, Germany, 1996.
(3) English, A. D. *Macromolecules* **1985**, *18*, 178.
(4) English, A. D.; Inglefield, P. T.; Jones, A. A.; Zhu, Y. *Polymer* **1998**, *39*, 309.
(5) Graf, R.; Heuer, A.; Spiess, H. W. *Phys. Rev. Lett.* **1998**, *80*, 5738.
(6) Graf, R.; Demco, D. E.; Hafner, S.; Spiess, H. W. *Solid State NMR* **1998**, *12*, 139.
(7) de Gennes, P. G. *J. Chem. Phys.* **1971**, *55*, 572.
(8) Doi, M.; Edwards, S. F. *The Theory of Polymer Dynamics*, Oxford University Press: Oxford, England, 1988.

(9) Hsieh, H. L.; Quirk, R. P. *Anionic Polymerization*; Marcel Dekker: New York, 1996.
(10) Flory, P. J. *J. Chem. Phys.* **1942**, *10*, 51.
(11) Huggins, M. *J. Phys. Chem.* **1942**, *46*, 151.
(12) Bates, F. S. *Science* **1991**, *251*, 898.
(13) Hashimoto, T. *Macromolecules* **1982**, *15*, 1548.
(14) Fetters, L. J.; Lohse, D. J.; Graessley, W. W. *J. Polym. Sci., B: Polym. Phys.* **1999**, *37*, 1023.
(15) Gottwald, J.; Demco, D. E.; Graf, R.; Spiess, H. W. *Chem. Phys. Lett.* **1995**, *243*, 314.
(16) Schnell, I.; Brown, S. P.; Low, H. Y.; Ishida, H.; Spiess, H. W. *J. Am. Chem. Soc.* **1998**, *120*, 11784.
(17) Lee, Y. K.; Kurur, N. D.; Helmle, M.; Johannessen, O. G.; Nielsen, N. C.; Levitt, M. H. *Chem. Phys. Lett.* **1995**, *242*, 304.
(18) Demus, D., Goodby, J., Gray, G. W., Spiess, H. W., Vill, V., Eds.; *Handbook of Liquid Crystals*; Wiley-VCH: New York, 1998.
(19) Zwetkoff, V. *Acta Physicochem. U.S.S.R.* **1939**, *10*, 55.
(20) Maier, W.; Saupe, A. *Z. Naturforsch.* **1958**, *13a*, 565.
(21) Ferry, J. D. *Viscoelastic Properties of Polymers*, 3rd ed.; Wiley: New York, 1980.
(22) Cohen-Addad, J. P. *J. Chem. Phys.* **1975**, *63*, 4880.
(23) Ball, R. C.; Callaghan, P. T.; Samulski, E. T. *J. Chem. Phys.* **1997**, *106*, 7352.
(24) Collignon, J.; Sillescu, H.; Spiess, H. W. *Colloid Polym. Sci.* **1981**, *259*, 220.
(25) Valic, S.; Deloche, B.; Gallot, Y.; Skoulios, A. *Polymer* **1995**, *36*, 3041.
(26) Callaghan, P. T.; Samulski, E. T. *Macromolecules* **1997**, *30*, 113.
(27) Callaghan, P. T.; Samulski, E. T. *Macromolecules* **1998**, *31*, 3693.
(28) Demco, D. E.; Hafner, S.; Fülber, C.; Graf, R.; Spiess, H. W. *J. Chem. Phys.* **1996**, *105*, 11285.
(29) Rouse, P. E. *J. Chem. Phys.* **1953**, *21*, 1272.
(30) Berry, G. C.; Fox, T. G. *Adv. Polym. Sci.* **1968**, *5*, 261.
(31) Flory, P. J. *Statistical Mechanics of Chain Molecules*; Interscience: New York, 1969.
(32) Faller, R.; Pütz, M.; Müller-Plathe, F. *Int. J. Mod. Phys. C* **1999**, *10*, 355.
(33) Milner, S. T.; McLeish, T. C. B. *Phys. Rev. Lett.* **1998**, *81*, 725.
(34) Kremer, K.; Grest, G. S. *J. Chem. Phys.* **1990**, *92*, 5057.
(35) Faller, R.; Heuer, A.; Müller-Plathe, F. *Macromolecules* **2000**, *33*, 6602.
(36) Rathgeber, S.; Willner, L.; Richter, D.; Brulet, A.; Farago, B.; Appel, M.; Fleischer, G. *J. Chem. Phys.* **1999**, *110*, 10171.
(37) Schleger, P.; Farago, B.; Lartigue, C.; Kollmar, A.; Richter, D. *Phys. Rev. Lett.* **1998**, *81*, 124.
(38) Kimmich, R.; Seitter, R. O.; Beginn, U.; Möller, M.; Fatkullin, N. *Chem. Phys. Lett.* **1999**, *307*, 147.
(39) Fischer, E.; Kimmich, R.; Beginn, U.; Möller, M.; Fatkullin, N. *Phys. Rev. E* **1999**, *59*, 4079.
(40) Fischer, E.; Kimmich, R.; Fatkullin, N. *J. Chem. Phys.* **1997**, *106*, 9883.
(41) Klein, P. G.; Adams, C. H.; Brereton, M. G.; Ries, M. E.; Nicholson, T. M.; Hutchings, L. R.; Richards, R. W. *Macromolecules* **1998**, *31*, 8871.
(42) Komlosh, M. E.; Callaghan, P. T. *J. Chem. Phys.* **1998**, *109*, 10053.
(43) Hamersky, M. W.; Tirrell, M.; Lodge, T. P. *Langmuir* **1998**, *14*, 6974.
(44) Schweizer, K. S. *J. Chem. Phys.* **1989**, *91*, 5822.
(45) Fuchs, M.; Schweizer, K. S. *Macromolecules* **1997**, *30*, 5133.
(46) Fuchs, M.; Schweizer, K. S. *Macromolecules* **1997**, *30*, 5156.
(47) Guenza, M.; Tang, H.; Schweizer, K. S. *J. Chem. Phys.* **1998**, *108*, 1257.
(48) Schmidt-Rohr, K.; Spiess, H. W. *Multidimensional Solid-State NMR and Polymers*; Academic: London, 1994.
(49) Spiess, H. W. In *NMR − Basic Priciples and Progress*, Diehl, P., Fluck, E., Kosfeld, R., Eds.; Springer-Verlag: Berlin, 1978; Vol. 15, p 55.
(50) Graf, R. *Hochauflösende Doppelquanten-NMR−Spektroskopie an Amorphen Polymeren*; Shaker-Verlag: Aachen, Germany, 1998.
(51) Graessley, W. W. *Adv. Polym. Sci.* **1982**, *47*, 67.
(52) Kulik, A. S.; Radloff, D.; Spiess, H. W. *Macromolecules* **1994**, *27*, 3111.
(53) Sotta, P.; Valic, S.; Deloche, B.; Maring, D.; Spiess, H. W. *Acta Polym.* **1999**, *50*, 205.
(54) Heuer, A. Unpublished results.
(55) Graf, R. Unpublished results.
(56) Baysal, C.; Erman, B.; Bahar, I.; Lauprêtre, F.; Monnerie, L. *Macromolecules* **1997**, *30*, 2058.
(57) Stöppelmann, G.; Gronski, W.; Blumen, A. *Polymer* **1990**, *31*, 1838.
(58) Dollase, T. *Influence of Rigid Confinements on Local Order and Chain Dynamics in Polymer Melts*; Logos-Verlag: Berlin, 2000.
(59) Graf, R.; Heuer, A. Unpublished results.
(60) Feigin, R. I.; Napper, D. H. *J. Colloid Interface Sci.* **1979**, *71*, 117.
(61) Murat, M.; Grest, G. S.; Kremer, K. *Europhys. Lett.* **1998**, *42*, 401.
(62) Heck, B.; Hugel, T.; Iijima, M.; Sadiku, E.; Strobl, G. *New J. Phys.* **1999**, *1*, 17.
(63) Hauser, G.; Schmidtke, J.; Strobl, G. *Macromolecules* **1998**, *31*, 6250.
(64) Hugel, T.; Strobl, G.; Thomann, R. *Acta Polym.* **1999**, *50*, 214.
(65) Dollase, T.; Spiess, H. W.; Gottlieb, M.; Yerushalmi-Rozen, R. *Crystallization of Semicrystalline Polymers: Influence of Physical and Chemical Cross-links*, to be submitted.

MA0013915